Calhoun: The NPS Institutional Archive

DSpace Repository

Theses and Dissertations | 1. Thesis and Dissertation Collection, all items

1958-06

Natural convection burnout in tubes closed at the bottom.

Neustel, Arthur Donald

Massachusetts Institute of Technology

http://hdl.handle.net/10945/26646

Downloaded from NPS Archive: Calhoun

http://www.nps.edu/library

Calhoun is the Naval Postgraduate School's public access digital repository for research materials and institutional publications created by the NPS community. Calhoun is named for Professor of Mathematics Guy K. Calhoun, NPS's first appointed -- and published -- scholarly author.

Dudley Knox Library / Naval Postgraduate School
411 Dyer Road / 1 University Circle
Monterey, California USA 93943

NPS ARCHIVE
1958.06
NEUSTEL, A.

NATURAL CONVECTION BURNOUT IN TUBES CLOSED AT THE BOTTOM

ARTHUR DONALD NEUSTEL

DUDLEY KNOX LIBRARY
NAVAL POSTGRADUATE SCHOOL
MONTEREY CA 93943-5101

NATURAL CONVECTION WITHOUT IN TUBES CLOSED AT THE BOTTOM

by

LIEUTENANT ARTHUR DONALD HEUSTEL, U.S.N.

B.S., U.S. Naval Academy

(1950)

SUBMITTED IN PARTIAL FULFILLMENT OF THE REQUIREMENTS FOR THE

DEGREE OF NAVAL ENGINEER AND FOR THE DEGREE OF

MASTER OF SCIENCE IN NAVAL ARCHITECTURE

AND MARINE ENGINEERING

at the

MASSACHUSETTS INSTITUTE OF TECHNOLOGY

June, 1958

Signature of Author _____

Department of Naval Architecture and
Marine Engineering, May 26, 1958

Certified by _____

Thesis Supervisor

Accepted by _____

Chairman, Departmental Committee
on Graduate Students

NPS ARCHIVE
1958.06
NEUSTEL, A.

Thesis
N444

ABSTRACT

NATURAL CONVECTION BURNOUT IN TUBES CLOSED AT THE BOTTOM

by

Arthur Donald Neustel

Submitted to the Department of Naval Architecture and Marine Engineering on May 26, 1958 in partial fulfillment of the requirements for the degree of Naval Engineer and the degree of Master of Science in Naval Architecture and Marine Engineering.

An investigation of the flow pattern and the heat flux immediately prior to and during burnout of vertical tubes closed at the bottom is made. This investigation is primarily concerned with the gradual "steady state" approach to burnout and is limited to tubes of 0.1805 inch and 0.061 inch I.D. Lengths of tube investigated vary from 4 inches to 107 5/8 inches.

The tubes used were heated by electrical current passing through the tube wall, and utilized the resistance of the tubes themselves for heating.

The flow pattern observed at the mouth of the tube was annular in all tubes used, with a core of vapor (steam), and with an annular downward flow of water next to the tube wall. Burnout is observed to occur at the bottom of the tube subject to certain limiting conditions.

A model for the flow is proposed, and calculations are made on this model. The model assumes fully developed laminar flow with heat transfer through the liquid layer by conduction alone. The inclusion of steam bubbles in the liquid phase is considered, with resultant decrease in density yielding results that approximate those observed. The model as originally proposed is considered to be an unsatisfactory model of the actual flow regime.

Thesis Supervisor: Peter Griffith
Title: Assistant Professor of Mechanical Engineering

37650

Chapter

ACKNOWLEDGMENTS

The author wishes to express his gratitude to Professor Peter Griffith for having devoted a great deal of his valuable time giving advice and encouragement during the development of this thesis.

The author also wishes to express his gratitude to Mr. Fred Johnson for his invaluable help in the assembly and replacement test sections and assistance in the design of the test section assembly.

TABLE OF CONTENTS

		Page
	Abstract	ii
	Acknowledgements	iii
	List of Figures	v
	Table of Symbols and Abbreviations	vi
I	Introduction	1
II	Procedure	3
	A. Equipment	3
	B. Operating Procedure	4
	C. Corrections for Heat Losses	6
III	Results	12
	A. General Observations	12
	B. Analytical Results	14
	C. Summary of Observed and Calculated Data	14
IV	Discussion of Results	17
	A. Variations in Data	17
	B. Comparison of Calculated and Observed Values	18
	C. Burnout	19
V	Conclusions	22
VI	Recommendations	23
VII	Appendix	24
	A. Analytical Model	25
	I Flow Regime and Proposed Model	25
	II Calculations	29
	B. Data Tables	35
	C. References	41

Page

LIST OF FIGURES

Figure		Page
I	General View of Test Section Assembly and Instrumentation	8
II	Test Section Assembly	9
III	Section View of Lower Part of Test Section Assembly	10
IV	Plan View of Bottom Plate of Test Section Assembly	10
V	Schematic Diagram of Equipment	11
VI	Plot of Temperature vs. Time Prior to Burnout	16
VII	Velocity of Steam-Water Interface as a Function of Interface Radius	32
VIII	Flow Rate of Liquid Phase as a Function of Interface Radius	33
IX	Velocity Profile for 0.1805" Test Section	34

Chapter		Page
I	[illegible]	1
II	[illegible]	7
III	[illegible]	17
IV	[illegible]	32
V	[illegible]	43
VI	[illegible]	55
VII	[illegible]	64
VIII	[illegible]	73
IX	[illegible]	84

SYMBOLS AND ABBREVIATIONS

I.D.	Inside Diameter
L	Length
r	Radius
T	Temperature (^{o}F)
V	Velocity
w	Mass rate of flow
z	Weight
ρ	Mass density
μ	Absolute viscosity of fluid
τ	Shear stress

Subscripts

v	Vapor or steam
l	Liquid phase
o	At the liquid-vapor interface
w	At the wall
i	Inside
o	Outside

I. INTRODUCTION

Burnout of tubes or coolant channels in a nuclear reactor or other heat source is a very serious condition. This condition, which is known as burnout, in which the coolant is completely, or nearly completely, removed from an area results in excessive temperatures in a localized or broad area and can result in the melting of the walls of the channel. The results of such melting in a nuclear reactor can be particularly severe since it may result in the radioactive contamination of the entire plant, or at least the primary coolant loop. Failures such as this may be caused by the plugging of a coolant channel by a foreign body or by coolant pump failure.

In the case of such failures, the only means of removing heat from the channel may be by natural convection. The case studied is the one in which the tube or coolant channel is completely closed at the bottom. This may be considered a limiting case in such failures and is usually the most severe. In this instance, the coolant which does reach the area susceptible to burnout must enter the tube from the top, and the heat removed must also be removed through the top of the tube or channel.

The nature of the flow and the maximum permissible heat flux in this case are not known, and yet the maximum heat flux that can be tolerated without burnout is of considerable practical importance in the design of such equipment. The problem of determining the flow pattern and the burnout heat flux is the one investigated in this paper. It is studied with a view to obtaining an insight into the mechanisms and phenomena that occur prior to, and during, burnout.

Previous investigations of these phenomena have been done at high

pressures, but these have proved of no value in this investigation. The difference in the density of steam between high pressures and atmospheric pressure results in differences in the flow and is the reason other studies have not been of value. No previous investigation of the burnout phenomenon at atmospheric pressure has been found.

Because previous investigations were of little value, this investigation was started with little idea of the nature of the flow or the results to be expected. This investigation was conducted entirely at atmospheric pressure for several reasons. The first of these is that by performing the experiments at atmospheric pressure, the apparatus and experiments are simplified. A second reason is that it is felt that by study of the phenomena at low pressure, insight may be gained into the nature of the problem which will facilitate other investigations at higher pressures. A third reason is that the results of this investigation may be useful directly in applications in which the pressure is low and at or near atmospheric pressure.

The nature of the problem is one in which the coolant, water in this study, enters the tube from the top. The steam, which is generated in the tube, must also leave by this same area. The resulting flow then is one of two-phase, counter-flow, in a tube with the additional complications of heat transfer and the change of state of the water. In addition, the only flow mechanism operating is that of natural convection.

II. [illegible]

A. Equipment

The equipment used to investigate the problem consisted of a vertical test section mounted below a reservoir. The upper end of the test section was silver-soldered into a small piece of copper conductor strap which was bolted to the bottom plate of the test assembly. The lower end of the test section was silver-soldered to a bottom connector plate which was also made of copper conductor strap. This bottom connector plate was then fastened to a section of Transite which, in turn, was bolted to a laboratory stand. The bottom plate of the reservoir was mounted on a rod which was clamped to the stand (Figures I and II).

The test section was heated by passing electrical current through the walls of the test section and using the resistance of the test section itself as the source of the heat. Power to the test section was supplied by a 15 kw motor-generator set with an output of up to 15 volts, 1000 amperes, direct current. Welding cable was used to connect the output terminals of the motor-generator set to the top and bottom connector plates of the test assembly and to the shunt across which the ammeter was connected.

The reservoir of the test assembly consisted of a section of 100 mm pyrex tubing about 8 inches long held between the top and bottom plates of the test assembly by stay bolts. (See Figures II, III, IV and V for details of the test assembly and schematic of the electrical circuit.)

Measurements of the power input were made by using a voltmeter

4. Conclusion

The experiments used to investigate the possible association of a mechanical load sensitive neuronal factor in pneumocytes. The system used in this study involving use of pneumocytes grown on flexible plastic substrata which could be deformed by the linear stretching. The system was to test whether changes due to deformation of a pulsing pneumocyte culture could alter the rate of sodium transport across it. The culture substratum grown on flat silicone rubber sheets. The rate of transport across the cultures was measured by a technique using radioactive sodium. The results of this study showed that the rate of sodium transport was not altered by the stretching of the substratum. The results of this study showed that the rate of sodium transport was not altered by the stretching of the substratum. The results of this study showed that the rate of sodium transport was not altered by the stretching of the substratum.

The experiments on the rate of sodium transport in a monolayer of pneumocytes grown on a flexible substratum which could be deformed by the linear stretching. The system was to test whether changes due to deformation of a pulsing pneumocyte culture could alter the rate of sodium transport across it. The culture substratum grown on flat silicone rubber sheets. The rate of transport across the cultures was measured by a technique using radioactive sodium. The results of this study showed that the rate of sodium transport was not altered by the stretching of the substratum. The results of this study showed that the rate of sodium transport was not altered by the stretching of the substratum.

The experiments on the rate of sodium transport in a monolayer of pneumocytes grown on a flexible substratum which could be deformed by the linear stretching. The system was to test whether changes due to deformation of a pulsing pneumocyte culture could alter the rate of sodium transport across it. The culture substratum grown on flat silicone rubber sheets. The rate of transport across the cultures was measured by a technique using radioactive sodium. The results of this study showed that the rate of sodium transport was not altered by the stretching of the substratum. The results of this study showed that the rate of sodium transport was not altered by the stretching of the substratum.

connected across the test section at the connector plates where the power leads were connected, and an ammeter connected across a shunt in one of the power cables to the assembly. The power to the test section was varied by controlling the current through the section by use of the rheostat on the motor-generator set.

Temperature measurements were made by the use of chromel-constantan thermocouples. These were installed on the test section after electrically insulating them from the test section with thin pieces of sheet mica by binding to the test section by means of asbestos string. They were positioned in various positions along the length of the various test sections. (Figure I shows one thermo-couple installed at the bottom of the test section.)

Two diameters of test sections were used in various lengths. Test sections of nickel tubing of 0.1805 inch inside diameter and 0.22 inch outside diameter were used in three lengths - 4, 8 and 107 5/8 inches. Stainless steel tubes of 0.061 inch inside diameter and 0.125 inch outside diameter were used in 4 and 8 inch lengths.

Because of the very low power inputs to the small diameter test sections, a coiled wire heating coil was placed in the reservoir to maintain the temperature of the water in the reservoir near boiling. This heating element was heated by using 115 volt a.c. current controlled with a variac of ten ampere capacity.

B. Operating Procedure

The equipment was mounted on a laboratory stand as shown in Figure I, and the motor-generator set was placed opposite it in such a position as to enable one person to reach any of the controls or meters without moving.

The operation of the equipment consisted of filling the reservoir with water to the desired depth (usually about two inches of water) and then energizing the motor-generator set. By closing the master switch on the control board of the motor-generator set, the test section was energized. The current through the test section was varied by means of the rheostat on the control board of the motor-generator set and was monitored by means of the ammeter in the test section leads.

After the test section had current flowing through it, the current was increased gradually until there were indications of burnout. Normally, however, the current through the test section was kept slightly below the current for burnout until the equipment and the water in the reservoir had sufficient opportunity to warm up, and then the "burned out" condition was approached very gradually.

As mentioned earlier, the small diameter test sections had such a small power requirement for burnout that an auxiliary heating element was placed in the reservoir to maintain the water temperature in the reservoir near boiling. The large test sections had sufficient power input to maintain the reservoir temperature at a reasonable level, and no auxiliary heater was used during these runs.

After the equipment was sufficiently warmed up, the current was gradually increased until some indication of burnout was seen. The current was actually increased in small steps, and the flow regime and temperatures were allowed to stabilize before the current was increased again. The length of time between these step changes of current varied with the test section in use, current and voltage indications, and the experience of the operator.

In each new test section the determination of the burnout current was arrived at by trial and error. With every section used, numerous indications of burnout were received before it was possible to approach the burnout condition from a reasonably steady state condition.

There were three methods used to indicate the approach to or the achievement of the burned-out state. The thermocouples were monitored, and temperatures were used as one of the indications. An increase of the wall temperature of the order of 20 to 30 degrees above the normal steady state temperature was used as an indication of burnout. This method was the primary method used in the long 107 inch test section and in the small, 0.061 inch diameter, test sections.

In the short test sections of 0.1805 inch diameter burnout was detected by thermocouples, too, but two other indications frequently proved valuable and were often noted first. These indications were the gradual drop off of current with a corresponding increase in voltage across the test section. This was caused by the increased resistance of the tube due to the higher temperatures of the tube wall. The other indication of burnout frequently noted was the change of color of the test section, first to a darker color, and then to red hot.

Temperature measurements themselves were used primarily as an indication of burnout, and their absolute value is not exact. The temperatures measured are an indication of the range of temperature on the tube wall and are useful only in this regard.

C. Corrections for Heat Losses

The measured power input into the test section includes the losses to the surrounding atmosphere and in the equipment itself. No correction was made in any case for any losses by conduction in either the top or

bottom connector plates.

The estimate of heat losses to the surrounding atmosphere by natural convection was made by the methods outlined by McAdams in reference 4. These losses are estimated to be of the order of 4 watts in the case of the 8 inch large diameter test section or approximately 2 percent of the heat input and a smaller percentage than this for the large diameter 4 inch test section. As a result of this estimate, no correction has been made for losses in the 4 and 8 inch 0.1805 inch I.D. test sections.

Similar calculations were made for the 0.061 inch I.D. test sections, and these have been applied as corrections to the data on these tubes. On the 107 inch section, however, the losses were estimated by heating the tube in the dry condition and measuring the power input to the tube required to maintain the tube at the same temperature observed during steady state operation.

The losses to the surrounding atmosphere because of the fin effect of the bottom connector plate are small, and are considered negligible in all cases except for the small diameter test sections. These losses are estimated to be approximately 1 watt. This correction was <u>not</u> made to the readings for any of the test sections, however.

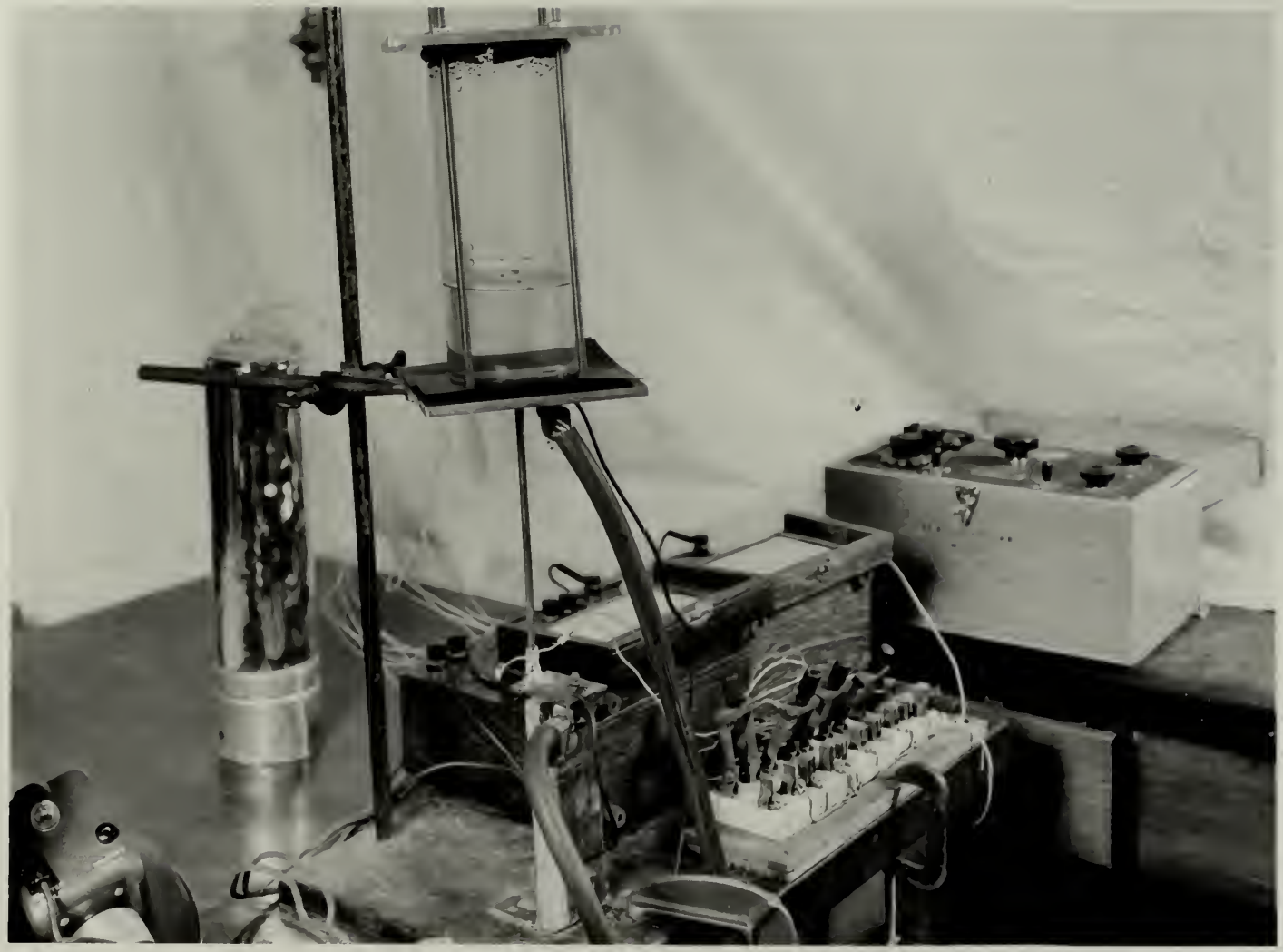

General View of Test Section Assembly and Instrumentation

Fig. 1

FIGURE II

TEST SECTION ASSEMBLY

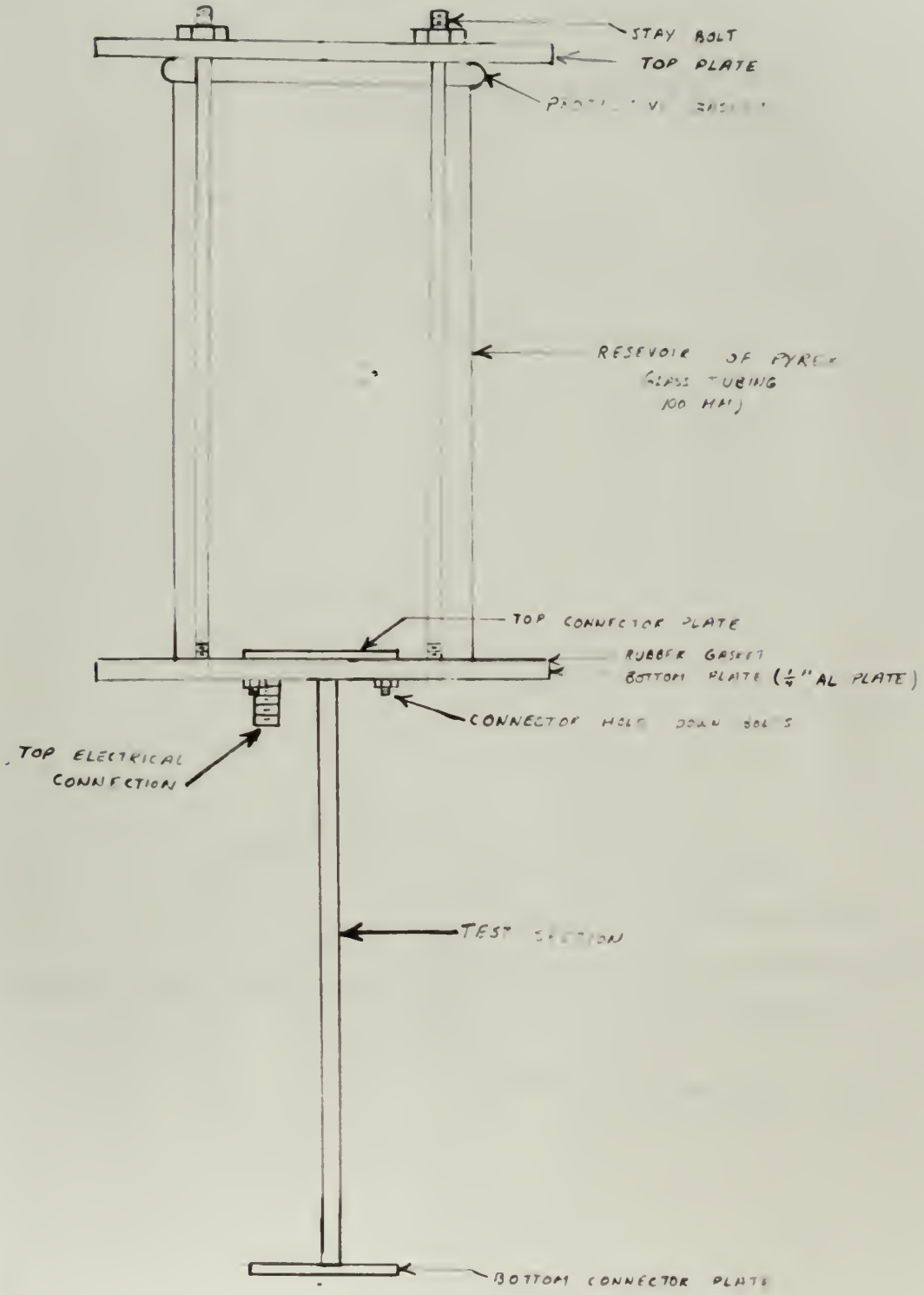

FIGURE III

SECTION VIEW OF LOWER PART
OF TEST SECTION ASSEMBLY

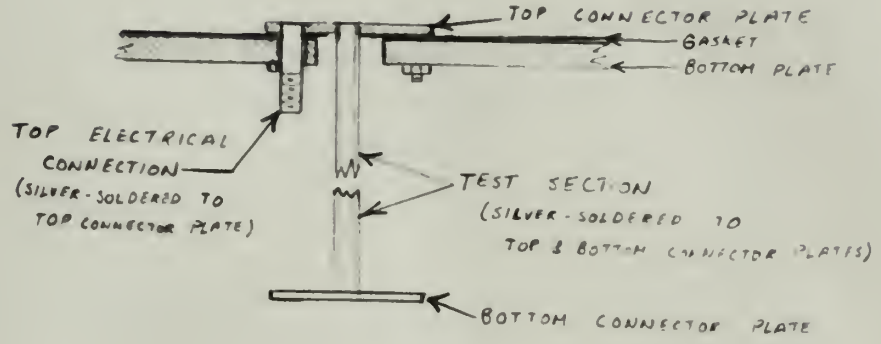
TOP CONNECTOR PLATE
GASKET
BOTTOM PLATE
TOP ELECTRICAL CONNECTION (SILVER-SOLDERED TO TOP CONNECTOR PLATE)
TEST SECTION (SILVER-SOLDERED TO TOP & BOTTOM CONNECTOR PLATES)
BOTTOM CONNECTOR PLATE

Not to scale
ADN 5/4/58

FIGURE IV

PLAN VIEW OF BOTTOM PLATE
OF TEST SECTION ASSEMBLY

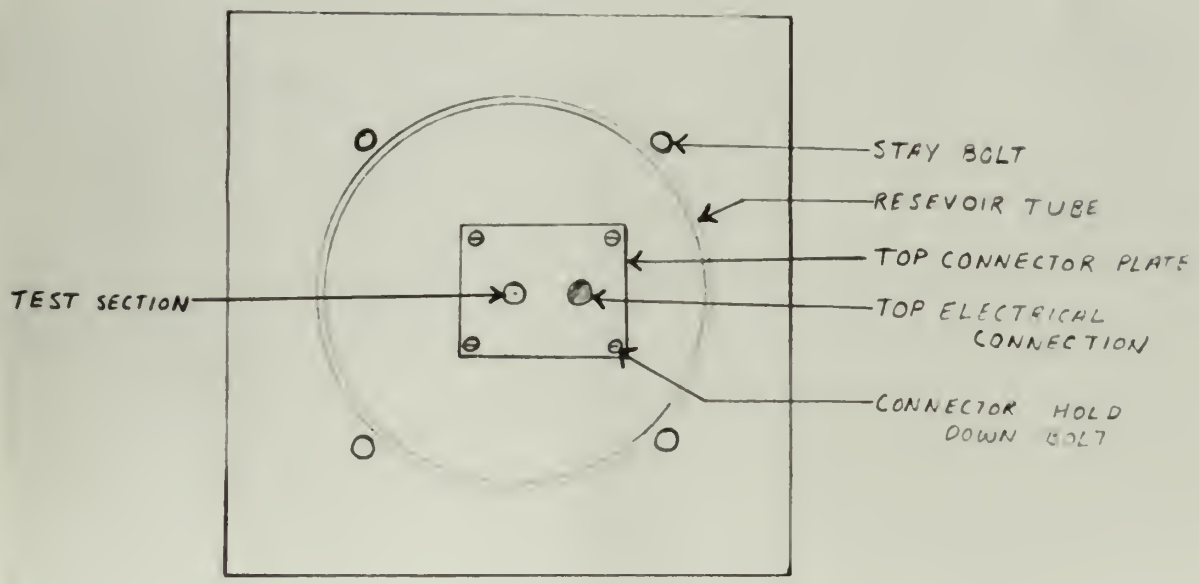

NOT TO SCALE
ADN 5/11/58

FIGURE V

SCHEMATIC DIAGRAM OF EQUIPMENT

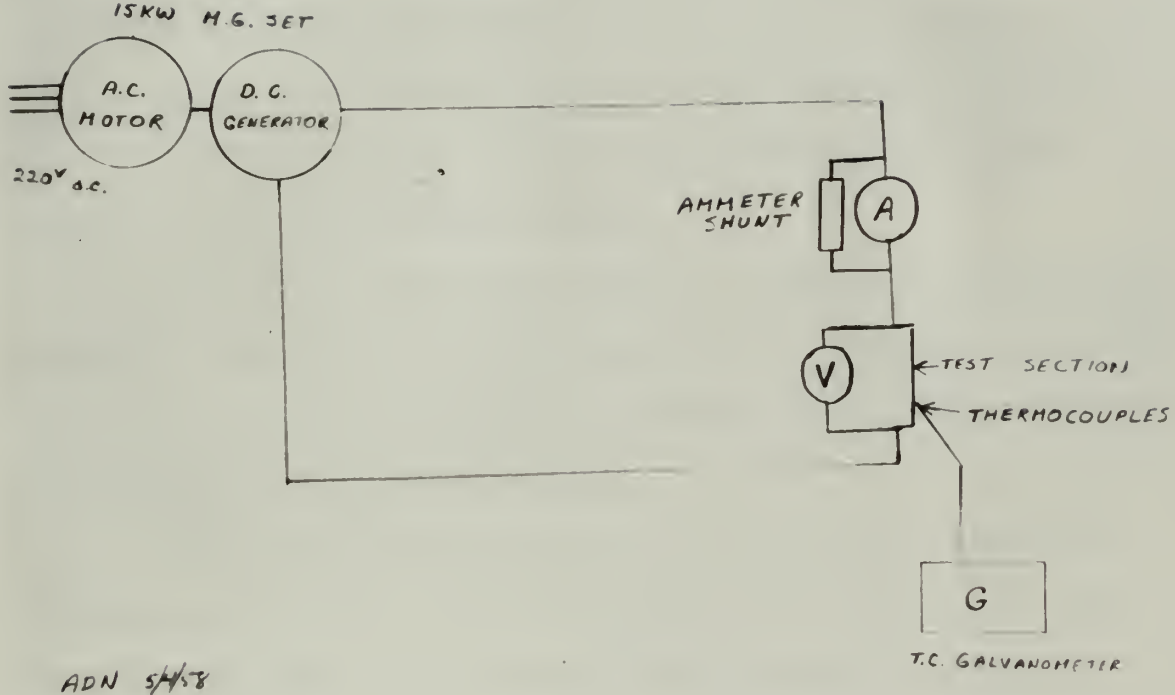

ADN S/H/S 8

III. RESULTS

A. General Observations

1. Observation of the mouth of the test sections by means of a stroboscopic light and by an ordinary incandescent lamp indicates that, without exception, the steady state flow prior to burnout at the mouth of the tube is one of an annular nature and consists of an annulus of water next to the tube wall, with a core of steam in the center of the test section. In no case was the core of steam observed to go below the end of the test section, although the growth and collapse of bubbles in the reservoir were observed.

2. During the steady state operation of the equipment, there was never any indication of the core of steam being interrupted with slugs of water, although this condition was observed while the equipment was warming up prior to the steady state.

3. During the initial heating of the test section, steam was emitted from the tube as individual bubbles with a sharp noise like steam pipe pounding. Small slugs of water were often ejected from the surface of the water in the reservoir completely over the top plate of the reservoir. This occurred in all the 0.1005 inch test sections and was noted particularly when there was 1½ to 2 inches of water in the reservoir. This means that these slugs or drops of water were ejected about 6½ inches (or more) from the surface of the water.

4. During the steady state operation, the only noise heard was a steady boiling noise which was attributed to the collapse of the steam bubbles in the reservoir.

5. During the steady state operation, the steam bubbles tended to

5. [illegible]

3. [illegible] [illegible] [illegible]

set a circular motion in the reservoir. The axis of the steam bubbles formed a cone with the axis of the bubble stream being of a maximum of about 15 degrees from the vertical. The motion of the axis of the bubbles was counterclockwise when viewed from above.

The shape of the bubbles in the reservoir when viewed with a stroboscopic light was of the general shape sketched below.

6. Burnout of the 0.1895 inch I.D. test sections occurred first at the bottom in all cases where the burnout was approached from a reasonably steady state. The location of burnout occurred farther up the tube in the cases when power inputs were appreciably larger than steady state or in the case of large power surges. In the case of very large surges, the location of burnout was unpredictable.

Burnout of the 0.061 inch I.D. tubes occurred between the bottom two thermocouples in both lengths of tubes tested. In no case was the burnout observed at the bottom first unless burnout had already occurred higher in the tube. On the 8 inch test section, this means burnout occurred between 4 3/4 inches and 7 1/2 inches from the top connector plate and between 2 and 4 inches from the top connector plate in the 4 inch test section.

7. Immediately prior to burnout, the temperature of the tube wall decreased before it increased to burnout. This phenomenon was observed in all the 0.1895 inch I.D. test sections, but it was not observed in

the small diameter sections. (See Figure VI.)

B. Analytical Results

A proposed model for the flow regime observed has been developed, and calculations based on it have been made. The proposed model is developed in detail in Appendix A, and the results of calculations based on it may be found following Appendix A.

C. Summary of Observed and Calculated Data

1. Average heat input and heat fluxes observed (corrected for estimated losses) for the various test sections are as follows: (See Appendix B for individual runs.)

Test Section Length	Diameter	Power Input (Watts)	Heat Flux (BTU/hr.ft.^{2})	Entrance to Test Section
4"	0.1805"	159	34,600	Square
8" (#1)	0.1805"	251	27,400	"
8" (#2)	0.1805"	200	21,800	"
8" (#2)	0.1805"	228	24,800	Rounded
107 5/8"	0.1805"	335	2,720	"
4"	0.061 "	6.9	4,420	"
8"	0.061 "	7.8	2,505	"

2. Calculation of the maximum weight rate of flow based on the model developed in Appendix A compares with the observed weight rates of flow as follows: (Observed rates are based on the heat input and the heat of vaporization.)

Test Section Length	Diameter	Observed Rate (# 1 hr.)	Calculated Rate (# 1 hr.) Water only	Water and steam bubbles	Entrance to Test Section
4"	0.1805"	0.559	5.30	1.31	Square
8" (#1)	0.1805"	0.881	"	"	"
8" (#2)	0.1805"	0.703	"	"	"
8" (#2)	0.1805"	0.801	"	"	Rounded
107 5/8"	0.1805"	1.18	"	"	"
4"	0.061 "	0.0243	0.0715	0.0174	"
8"	0.061 "	0.0274	0.0715	0.0174	"

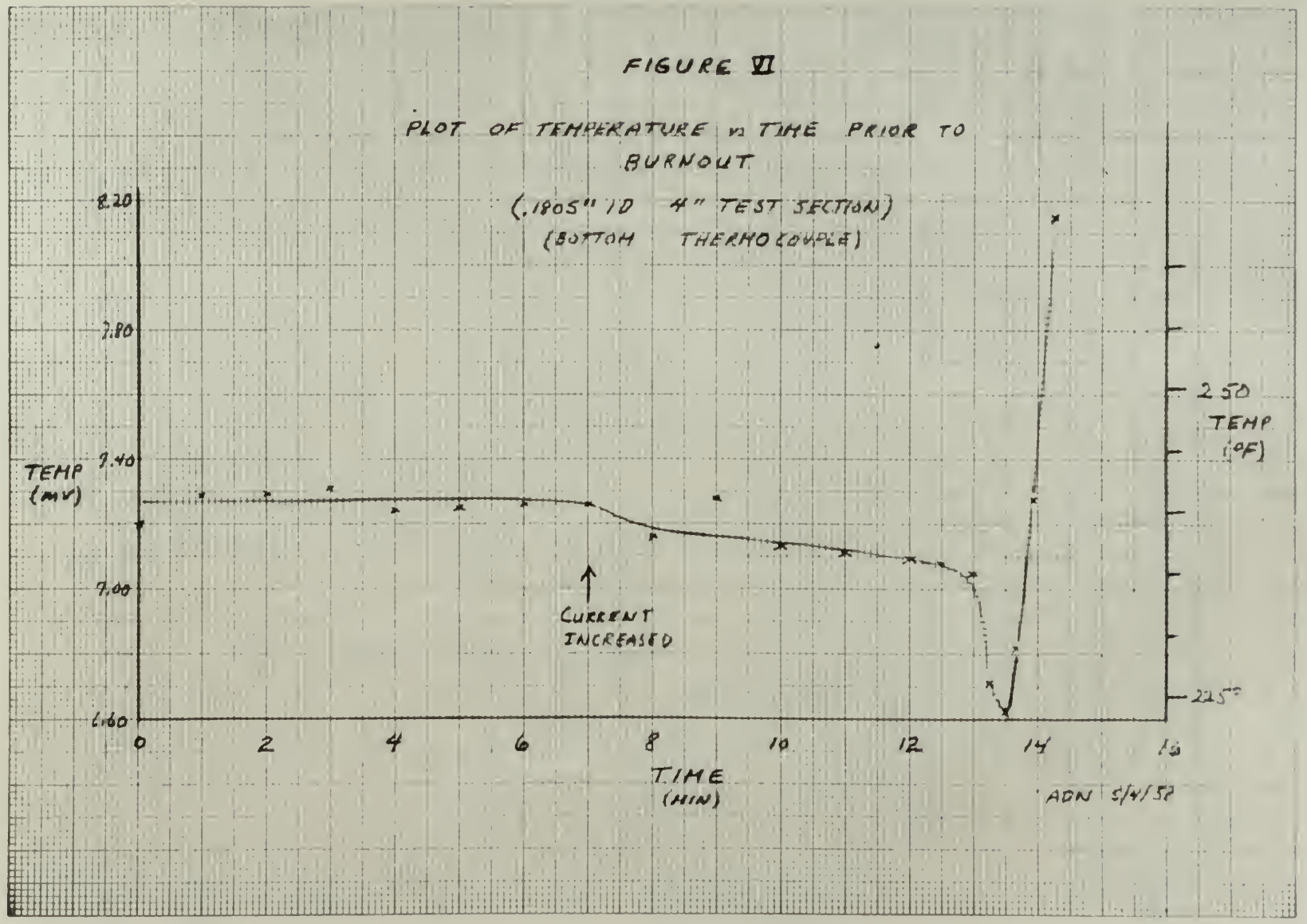
FIGURE VI
PLOT OF TEMPERATURE vs TIME PRIOR TO BURNOUT
(.1805" ID 4" TEST SECTION)
(BOTTOM THERMOCOUPLE)
8.20
7.80
7.40
7.00
6.60
TEMP (mv)
0
2
4
6
8
10
12
14
16
TIME (MIN)
CURRENT INCREASED
250
TEMP (°F)
225°
ADN 5/4/52

IV. DISCUSSION OF RESULTS

A. Variations in Data

There are several instances in which there are discrepancies or variations in the data. Several factors account for them. For example, the experience of the author in operating the assembly is responsible for some of the variations.

The temperature measurements were intended only as an indication of burnout and of the general temperature level of the tube. The temperatures shown are known to not be precise, and there are several sources of error. The variation in the thickness of the mica insulator is a source of some error in the readings. A correction of 3°F has been made to all temperature readings in Appendix B to correct for the effect of the layer of mica. Another source of variation is the tightness with which the thermocouples were bound to the test section. This error could be of the order of magnitude of 10°F, when the thermocouples were installed by different people. It is not felt that the variation between thermocouples due to installation on any one test section or of any one thermocouple on a test section has errors of this magnitude. Such errors are estimated to be of the order of 1°F. Temperatures on any single test section were consistent with the others on the same test section, during steady state operation, and followed a consistent pattern with those on other test sections. As a result of the difference in temperatures from thermocouples installed by different persons, a correction of 0.35 mv has been applied to the data in Appendix B as noted. This correction is based on installation of the thermocouples on the same test section by the persons involved.

The variation of the power input to two identical test sections and of the weight rates of flow to these test sections (the 8 inch long 0.1805 inch I.D. square entrance sections) is attributed to several factors. One is the experience of the author in operating the assembly. Another is possible differences in the condition of the test section inner surface and the entrance to the test sections. As reshaping of the entrance to the second of these 8 inch, 0.1805 inch I.D. test sections indicates, the entrance effect may cause some variation in results, since an increase of 14 percent in power input was obtained by reshaping the entrance to this section.

B. Comparison of Calculated and Observed Values

The observed values of weight rate of flow and the power input to the various test sections increased with increasing length of the test section. This indicates that the limiting condition of the flow pattern has not been imposed by the considerations proposed in the model, but other conditions impose limitations on the flow. As indicated in Appendix A, the assumption has been made that the heat transfer is accomplished by conduction of heat through the liquid layer. This may not be true, because there may be bubbles which interrupt the flow on the wall. Bubbles could cut down the area in which water is flowing, as well as resulting in different conditions for vaporization in the immediate area. The combination of these factors appears consistent - the longer tubes had lower wall temperatures, and hence logically would have fewer bubbles on the wall if there are, in fact, these bubbles. This would mean that the weight rate of flow would be larger, which is borne out by the observation.

The consideration of the fact that there may be bubbles entrained

in the water flowing downward in the annulus or adjacent to the wall led to the calculations based on a reduced density for the water flowing down the wall. The calculation, outlined in Appendix A, assumes that the mixture flowing down the wall is a mixture of water at saturation and contains spherical bubbles of steam as closely packed as possible. This results in a reduction of the density flowing downward to approximately 1/4 of its previous value, and only a small change in the interface radius for maximum flow rate. The calculated flow rate is then somewhat nearer the observed value. In the 0.061 inch I.D. sections, the observed flow rates are between these two calculated values and indicates that the model may be a logical one if proper allowance can be made for the density and viscosity of the liquid phase in the test section. In the larger test sections the same tendencies are observed, and it appears that if long enough test sections of this size could be tested that the flow rate would approach a value somewhat between the two values calculated. In the 0.1805 inch I.D. test sections used, it appears that the effective density for this model is less than that assumed for calculation purposes. The results of these runs are considered to be inconclusive, although they do not rule out the model proposed. If bubbles of steam are fixed in position along the tube wall, thus reducing the effective density, the flow down the wall would be disrupted. Then heat transfer no longer would be transferred by conduction alone, and the model proposed would not be adequate.

C. Burnout

The location of the first portion of the tube to burnout was consistently at the bottom of the tube in the large 0.1805 inch I.D. test sections. In the small 0.061 inch I.D. test sections, however, it

occurred somewhat higher in the tube. Insufficient runs were made on the small diameter test sections to ascertain whether the data on burnout location obtained was accurate for the limiting steady-state approach to burnout. On the shorter of the small sections, it is felt that insufficient time was given for the equipment to adequately warm up and that the burnout would probably have occurred at the bottom of the test section had longer runs been made. It is hypothesized that there is a portion of the tube filled with water at the bottom, and that there is a time delay required for this to be evaporated or boiled out before the true steady state is attained. Insufficient time was allowed for this process to take place in the 4 inch 0.061 inch I.D. test section with the result that burnout may have occurred higher in the tube than under the true steady state condition. In addition, the fin effect of the bottom connector plate increases heat losses in this area and retards this process.

In the case of the 8 inch small diameter section, much longer runs were made, and it is believed that the burnout location may be correct. The exact location of burnout was impossible to determine in the small diameter tubes, because the only indication of burnout was the thermocouple readings, and these were spaced at intervals of about two inches. The theoretical "critical" length in this size tube based on the model proposed in Appendix I and an assumed tube wall temperature of 222°F is 5.25 inches from the top connector plate. This is consistent with the observations in the results that burnout occurred between 4 3/4 inches and 7 1/2 inches from the top of the test section.

In the large diameter test sections, the calculated "critical" length is about 18 feet (based on a 227°F wall temperature), and there

was no opportunity or space to test tubes longer than the section of about 9 feet that was tested. As mentioned earlier, in all of these sections burnout was at the bottom of the tube. This is consistent with the model proposed in Appendix A.

The variation of the temperature immediately prior to burnout as illustrated in Figure VI was observed in all lengths of 0.1305 inch test sections. It was not observed in the small test sections, because the thermocouples were not directly on the burnout location and, in addition, the tube walls had a very large heat capacity. It is believed that this same phenomenon occurs in the small tube and could be observed if a tube with thinner walls, properly instrumented, were used. This variation of temperature is probably caused by the thinning down of the liquid layer along the wall just prior to burnout. Thinning of the liquid layer would improve the heat transfer according to the model assumed and thus increase the vaporization. This would result in a lowering of the temperature in the local area where burnout then commences and could account for the behavior shown.

V. CONCLUSIONS

1. The flow configuration at the mouth of the tube in the steady state at somewhat less than the burnout heat flux is of an annular nature with the liquid water flowing down the wall, and a continuous vapor core flowing up the center.
2. Because of the variation between model and observations, it is concluded that the model proposed in Appendix A is not an adequate representation of the flow that exists prior to burnout.
3. Burnout of tubes closed at the bottom, when approached from the steady state, normally occurs at the bottom of the tube. Burnout may occur further up the tube due to either end conduction or transient effects.

5. [illegible] to [illegible] already [illegible] at [illegible]. [illegible] [illegible] [illegible]

VI. [illegible]

1. That further investigations be conducted in such a manner that the flow inside of the tube can be observed. This might be accomplished in some manner such as viewing the flow through the bottom of the tube by inserting a transparent plug in the bottom.
2. That further investigations be done with a small diameter tube which has been more accurately and completely instrumented with thermocouples. It is also recommended that the tube wall be kept thin on future work with small tubes to minimize the effect of wall heat capacity.

APPENDIX A

Analytical Model

I. Flow Regime and Proposed Model

On the basis of the observed flow pattern, a model was proposed and calculations were done based on this model as follows. Observations indicated without question that the flow regime at the mouth of the tube in the steady state was one of an annular nature with the water flowing down the tube wall and a core of steam up the center.

The model proposed is based on the following assumptions:

(1) That the flow of both the steam and water is laminar in nature.

(2) That the weight rates of flow of water and steam are equal.

(3) That the interface of the two phases in the limiting region is a plane cylindrical surface, and the following conditions exist at the interface.

(a) The shear force in the liquid is equal to the shear force in the steam.

(b) The velocity of the steam is the same as the velocity water at this point.

(4) That the flow reaches the limiting condition when the weight rate of flow (of either steam or water, since they are equal) is a maximum.

(5) That all heat is transferred through the liquid layer by conduction and that all evaporation occurs at the interface.

(6) That the water and steam phases are at saturated conditions.

A. Development of Equations for this Model

The development of the equations for the proposed flow scheme is

[illegible]

[illegible]

1. [illegible]

[illegible]

[illegible]

[

shown below, using the assumptions outlined above.

The water flowing down the tube wall is assumed rather thin, so that a slab approximation is made for the force balance. Further, it is assumed that there is no pressure differential on the element of volume (i.e., the pressure is approximately constant throughout the length of the test section). Setting up a force balance on an elemental volume of water of length L, height dz and width dr, we have:

$$L\rho_\ell dz\, dr = \tau_i L\, dz - \tau_{(i+dr)} L\, dz \tag{1}$$

where

$$\tau_i = \mu_\ell \frac{dV_\ell}{dr}$$

and $$\tau_{(i+dr)} = \mu_\ell\left[\frac{dV_\ell}{dr} + \frac{d}{dr}\frac{dV_\ell}{dr}\, dr\right]$$

Substitution of these in equation (1) and canceling terms gives

$$\frac{d^2V_\ell}{dr} = \frac{\rho_\ell}{\mu_\ell}$$

Integrating twice,

$$V_\ell = \frac{\rho_\ell}{2\mu_\ell} r^2 + C_1 r + C_2 \tag{2}$$

Substitution of the boundary conditions that $V_\ell = o$ when $r = r_w$ and that $V_\ell = V_o$ when $r = r_o$ gives values for C_1 and C_2

$$C_1 = \left[V_o - \frac{\rho_\ell}{2\mu_\ell}(r_o^2 - r_w^2)\right]\frac{1}{r_o - r_w} \tag{3}$$

and $$C_2 = -\frac{\rho_\ell}{2\mu_\ell} r_w^2 - \frac{r_w}{r_o - r_w}\left[V_o - \frac{\rho_\ell}{2\mu_\ell}(r_o^2 - r_w^2)\right] \tag{4}$$

and $V_\ell = \frac{\rho_\ell}{2\mu_\ell}(r^2 - r_w^2) + \frac{(r - r_w)}{r_o - r_w}\left[V_o - \frac{\rho_\ell}{2\mu_\ell}(r_o^2 - r_w^2)\right]$

The weight rate of flow of the liquid is

$$w_\ell = L\rho_\ell \int_{r_o}^{r_w} V_\ell \, dr \tag{5}$$

where L is the length of the elemental area of width dr and is substituted for later as the mean circumference of the annulus of water.

Integration of (5) gives

$$w_\ell = L\rho_\ell\left[\frac{\rho_\ell}{12\mu_\ell}(r_o - r_w)^3 + \frac{V_o}{4}(r_w^2 - r_o^2)\right] \tag{6}$$

Substituting $L = \frac{r_o + r_w}{2}(2\pi)$ and rearranging

$$\frac{w_\ell}{2\pi\rho_\ell} = \frac{r_o + r_w}{2}\left[\frac{\rho_\ell}{12\mu_\ell}(r_o - r_w)^3 + \frac{V_o}{4}(r_w^2 - r_o^2)\right]$$

Turning now to the vapor or steam phase, assuming that the velocity distribution is that of fully developed parabolic flow, we have

$$V_v = \frac{C_1 r^2}{2} + C_2 r + C_3 \tag{7}$$

At $r = o$, $\frac{d V_v}{dr} = o$ and therefore $C_2 = o$

Since the shear forces must be equal at the interface of the liquid and steam, we have the condition

$$\mu_v\left(\frac{d V_v}{dr}\right)_{r_o} = \mu_\ell\left(\frac{d V_\ell}{dr}\right)_{r_o} \tag{8}$$

$$\left[\frac{\partial^2 \psi}{\partial x^2} + \frac{\partial^2 \psi}{\partial y^2}\right] = \frac{\partial}{\partial x}\left(\frac{\partial \psi}{\partial x}\right) + \frac{\partial}{\partial y}\left(\frac{\partial \psi}{\partial y}\right)$$

(42)

Using the above relation, we shall now determine the

$$\psi = \frac{\partial^2 \psi}{\partial x^2} + \frac{\partial^2 \psi}{\partial y^2} = 0$$

(43)

we have

$$\left[\frac{\partial^2 \psi}{\partial x^2} + \frac{\partial^2 \psi}{\partial y^2}\right] = \frac{\partial}{\partial x}\left[\frac{\partial \psi}{\partial x}\right] + \frac{\partial}{\partial y}\left[\frac{\partial \psi}{\partial y}\right]$$

Therefore from (1) the relation (43) becomes

$$\left[\frac{\partial^2 \psi}{\partial x^2} + \frac{\partial^2 \psi}{\partial y^2}\right] = \frac{\partial}{\partial x}\left[\frac{\partial \psi}{\partial x}\right] + \frac{\partial}{\partial y}\left[\frac{\partial \psi}{\partial y}\right]$$

(44)

Substituting the value of ψ from (2) in (44)

$$\left[\frac{\partial^2 \psi}{\partial x^2} + \frac{\partial^2 \psi}{\partial y^2}\right] = \frac{\partial}{\partial x}\left[\frac{\partial}{\partial x}(f(x) - \frac{\partial^2 \phi}{\partial x^2} + \frac{\partial^2 \phi}{\partial y^2})\right] + \frac{\partial}{\partial y}\left[\frac{\partial}{\partial y}(f(x) - \frac{\partial^2 \phi}{\partial x^2} + \frac{\partial^2 \phi}{\partial y^2})\right]$$

(45)

Differentiating (45) given

$$\left[\frac{\partial^2 \psi}{\partial x^2} + \frac{\partial^2 \psi}{\partial y^2}\right] = \frac{\partial}{\partial x}\left[\frac{\partial}{\partial x}(f(x) - \frac{\partial^2 \phi}{\partial x^2} + \frac{\partial^2 \phi}{\partial y^2})\right] + \frac{\partial}{\partial y}\left[\frac{\partial}{\partial y}(f(x) - \frac{\partial^2 \phi}{\partial x^2} + \frac{\partial^2 \phi}{\partial y^2})\right]$$

(46)

Differentiating (46) given

$$\left[\frac{\partial^2 \psi}{\partial x^2} + \frac{\partial^2 \psi}{\partial y^2}\right] = \frac{\partial}{\partial x}\left[\frac{\partial}{\partial x}(f(x) - \frac{\partial^2 \phi}{\partial x^2} + \frac{\partial^2 \phi}{\partial y^2})\right] + \frac{\partial}{\partial y}\left[\frac{\partial}{\partial y}(f(x) - \frac{\partial^2 \phi}{\partial x^2} + \frac{\partial^2 \phi}{\partial y^2})\right]$$

(47)

where ψ is the stream function and ϕ is the velocity potential.

Equation (47) is the required differential equation of the stream function ψ for flow through porous media.

Substitution in equation (8)

$$C_1 = \frac{\mu_\ell}{\mu_v} \frac{1}{r_o} \left[\frac{V_o}{r_o - r_w} + \frac{\rho_\ell}{2\mu_\ell} (r_o - r_w) \right] \tag{9}$$

Using the condition that $V_v = V_o$ at $r = r_o$ gives

$$C_3 = V_o - \frac{\mu_\ell}{2\mu_v} r_o \left[\frac{V_o}{r_o - r_w} + \frac{\rho_\ell}{2\mu_\ell} (r_o - r_w) \right] \tag{10}$$

Substitution of (9) and (10) in equation (7) gives

$$V_v = \frac{\mu_\ell}{2\mu_v} \frac{r^2 - r_o^2}{r_o} \left[\frac{V_o}{r_o - r_w} + \frac{\rho_\ell}{2\mu_\ell} (r_o - r_w) \right] + V_o \tag{11}$$

The weight rate of flow of the vapor is

$$w_v = \int_0^{r_o} 2\pi \rho_v r V_v \, dr$$

Substituting, integrating, and evaluating the integral yields:

$$\frac{w_v}{2\pi\rho_v} = \frac{\rho_\ell}{16\mu_v} r_o^3 (r_w - r_o) + V_o \left[\frac{r_o^2}{2} - \frac{\mu_\ell r_o^3}{8\mu_v (r_o - r_w)} \right] \tag{12}$$

The weight rates of flow of vapor and of liquid must be equal under assumption 2. Because of the sign convention chosen $w_v = -w_\ell$, as may be easily seen in the case when $V_o = 0$, since $r_o < r_w$.

Equating the weight rates of flow and solving for V_o as a function of r_o gives:

$$V_o = \frac{(r_o - r_w) \left[\frac{\rho_v}{16\mu_v} r_o^3 - \frac{\rho_\ell}{24\mu_\ell} (r_o - r_w)^2 (r_w + r_o) \right]}{\frac{r_w^2 - r_o^2}{4} + \frac{\rho_v}{\rho_\ell} \left(\frac{r_o^2}{2} - \frac{\mu_\ell}{8\mu_v} \frac{r_o^3}{r_o - r_w} \right)} \tag{13}$$

The maximum flow rate can then be determined by taking the derivative of w_ℓ (or w_v) with respect to r_o and setting it equal to 0.

$$\frac{dw_\ell}{dr_o} = \frac{\rho_\ell}{24\mu_\ell}\left[(r_o-r_w)^3 + 3(r_w+r_o)(r_o-r_w)^2\right] - \frac{V_o r_o}{2} + \frac{r_w^2-r_o^2}{4}\frac{dV_o}{dr_o} \qquad (14)$$

and if V_o is $= \frac{N}{D}$

$$\frac{dV_o}{dr_o} = \frac{(r_o-r_w)\left[\frac{3\rho_v}{16\mu_v} r_o^2 - \frac{\rho_\ell}{24\mu_\ell}\left\{2(r_o^2 - r_w^2) + (r_o - r_w)^2\right\}\right]}{D} +$$

$$\frac{r_o-r_w\left[\frac{\rho_v}{16\mu_v} r_o^3 - \frac{\rho_\ell}{24\mu_\ell}(r_o - r_w)^2(r_w + r_o)\right]}{D}$$

$$- \frac{N}{D^2}\left[-\frac{r_o}{2} + \frac{\rho_v}{\rho_\ell}\left\{r_o - \frac{\mu_\ell}{\mu_v}\frac{3(r_o - r_w) r_o^2 - r_o^3}{(r_o - r_w)^2}\right\}\right] \qquad (15)$$

II. Calculations

Because of the complex nature of these equations, it was determined that the solution could be most easily obtained by substitution of various values of r_o in the equations and plotting the resulting values of the velocity at the interface, the derivative of the weight rate of flow, and the weight rate of flow. Curves of V_o and $\frac{w_\ell}{2\pi\rho_\ell}$ as a function of the interface radius are attached as Figures VII and VIII for the 0.1805 inch I.D. test section. Curves of $\frac{w_\ell}{2\pi\rho_\ell}$ for the small diameter test section are also shown in Figure VIII. Curves are shown for the case where the water phase is assumed to be solid water at saturated conditions. In addition, there are plots of the $\frac{w_\ell}{2\pi\rho_s}$ for the assumed water-steam mixture plotted on Figure VIII. (See

$$\frac{\partial \mathcal{L}}{\partial \dot{q}_i} = \frac{\partial}{\partial \dot{q}_i}\left[\tfrac{1}{2}m(\dot{x}^2+\dot{y}^2+\dot{z}^2) - V(x,y,z)\right] = \frac{\partial}{\partial \dot{q}_i}\left[\tfrac{1}{2}m(\dot{x}^2+\dot{y}^2+\dot{z}^2)\right] - \frac{\partial V}{\partial x}\frac{\partial x}{\partial \dot{q}_i} \qquad (12)$$

$$\frac{\partial \mathcal{L}}{\partial \dot{q}_i} = \frac{\partial}{\partial \dot{q}_i}\left[\tfrac{1}{2}m(\dot{x}^2+\dot{y}^2+\dot{z}^2)\right] - \frac{\partial V}{\partial x}\frac{\partial x}{\partial \dot{q}_i}$$

$$\frac{\partial \mathcal{L}}{\partial \dot{q}_i} = \frac{\partial}{\partial \dot{q}_i}\left[\tfrac{1}{2}m(\dot{x}^2+\dot{y}^2+\dot{z}^2)\right] - \frac{\partial V}{\partial x}\frac{\partial x}{\partial \dot{q}_i}$$

$$\frac{\partial \mathcal{L}}{\partial \dot{q}_i} = \frac{\partial}{\partial \dot{q}_i}\left[\tfrac{1}{2}m(\dot{x}^2+\dot{y}^2+\dot{z}^2)\right] - \frac{\partial V}{\partial x}\frac{\partial x}{\partial \dot{q}_i} \qquad (13)$$

11. [illegible]

[illegible] is [illegible] [illegible] [illegible]

following discussion regarding the mixture assumptions.)

A velocity profile has been drawn for the large diameter test sections on the basis of the original assumptions and is attached as Figure IX. This is drawn to a single scale, with an insert showing the velocity profile in the water phase to a larger scale.

The values of the constants used for the calculations are tabulated below as taken from references 3 and 4, from actual test sections, and as calculated. (The use of these values requires conversion factors for units including g, acceleration due to gravity.)

ρ_ℓ = 59.9 lb./ft.^{3} r_w = 0.09025" (large test section)

ρ_v = 0.0373 lb./ft.^{3} r_w = 0.0305" (small test section)

μ_v = 8.38 x 10^{-6} lb.sec./ft.^{2} ρ_z = 15.6 lb./ft.^{3} (for mixture)

μ_ℓ = 1.75 x 10^{-4} lb.sec./ft.^{2} μ_z = 1.69 x 10^{-4} lb.sec./ft.^{2} (for mixture)

After the results of these calculations on the basis of the original assumptions were completed, it was decided to perform the calculations based on this model on the assumption that the liquid phase contained bubbles of steam. As a basis for this calculation, it was assumed that the steam bubble mixture density would be approximated as a mixture of spheres of steam as tightly packed as possible. The resulting mixture is 74 percent steam (by volume) and 26 percent saturated water, and the density resulting is 15.6 lb./ft.^{3} as noted above. For this calculation, it was also assumed that the viscosity of the mixture was a linear function, by weight, of the viscosity of the components with the resulting viscosity being 1.69 x 10^{-4} lb.sec./ft.^{2}.

In order to estimate the "critical" length expected, the value of the maximum weight rate of flow was calculated as outlined above. This

was then multiplied by the heat of vaporization to obtain the heat input necessary to evaporate sufficient steam to provide the weight rate of flow. On the basis of observed wall temperature in the first test sections, it was assumed that approximately a 15° temperature difference existed across the liquid phase inside the tube (10°F for the small diameter sections). On the basis of these temperature differences, the thermal conductivity of water as given in reference 4, and the thickness of the liquid layer, the length of tube necessary to give this heat flow was calculated. The calculated "critical" lengths are 18 feet for the large test sections and 5.25 inches for the small test sections, based on the original assumption of an annulus of solid water.

It should be noted that if the temperature difference is smaller, the result is that the "critical" length becomes longer. Thus, on this basis it should be possible to make the burnout occur at the bottom of nearly any tube if the power input per unit length is sufficiently small.

FIGURE VII

VELOCITY OF STEAM-WATER INTERFACE AS A FUNCTION OF INTERFACE RADIUS (FOR .1605" ID TUBE)

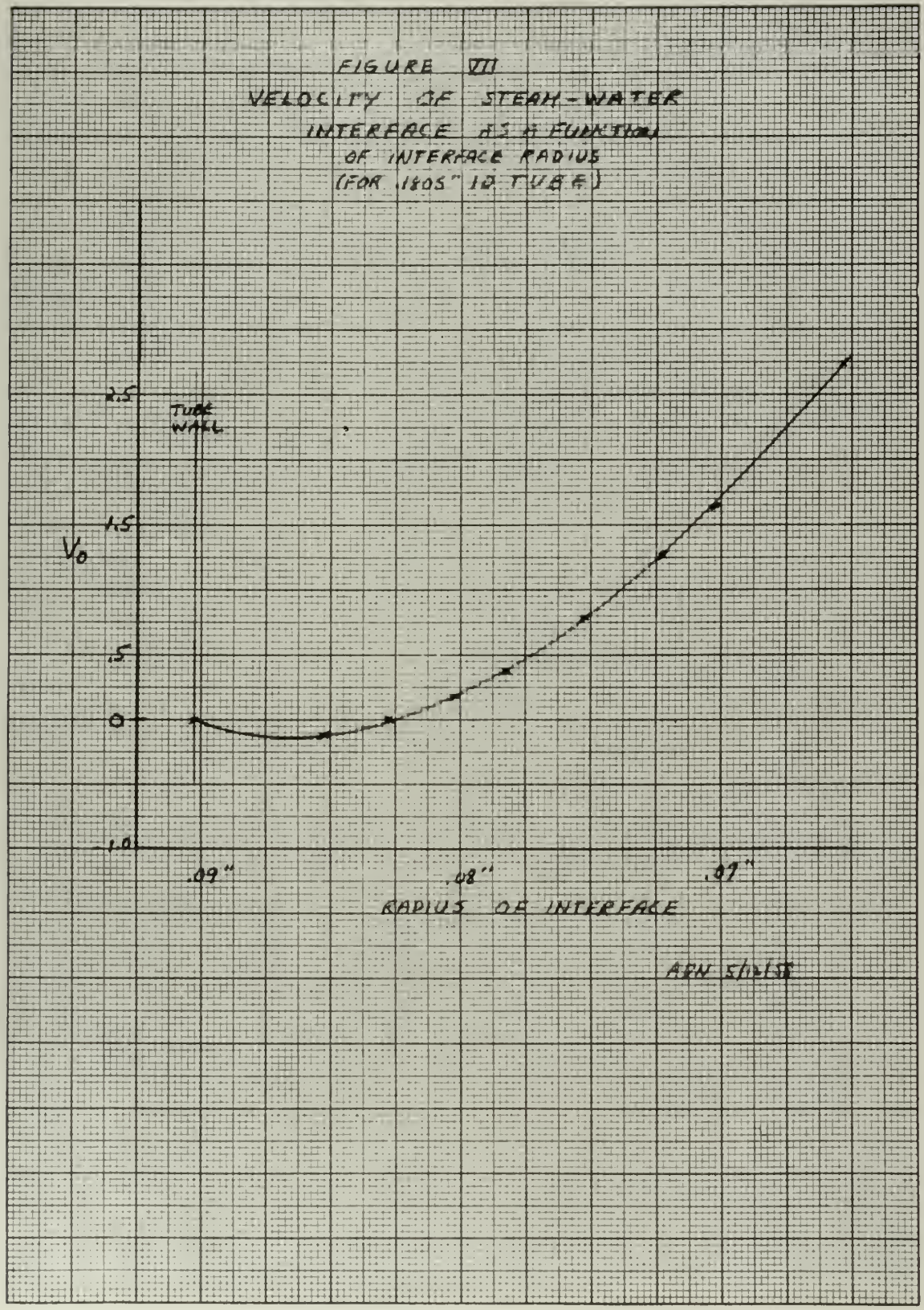

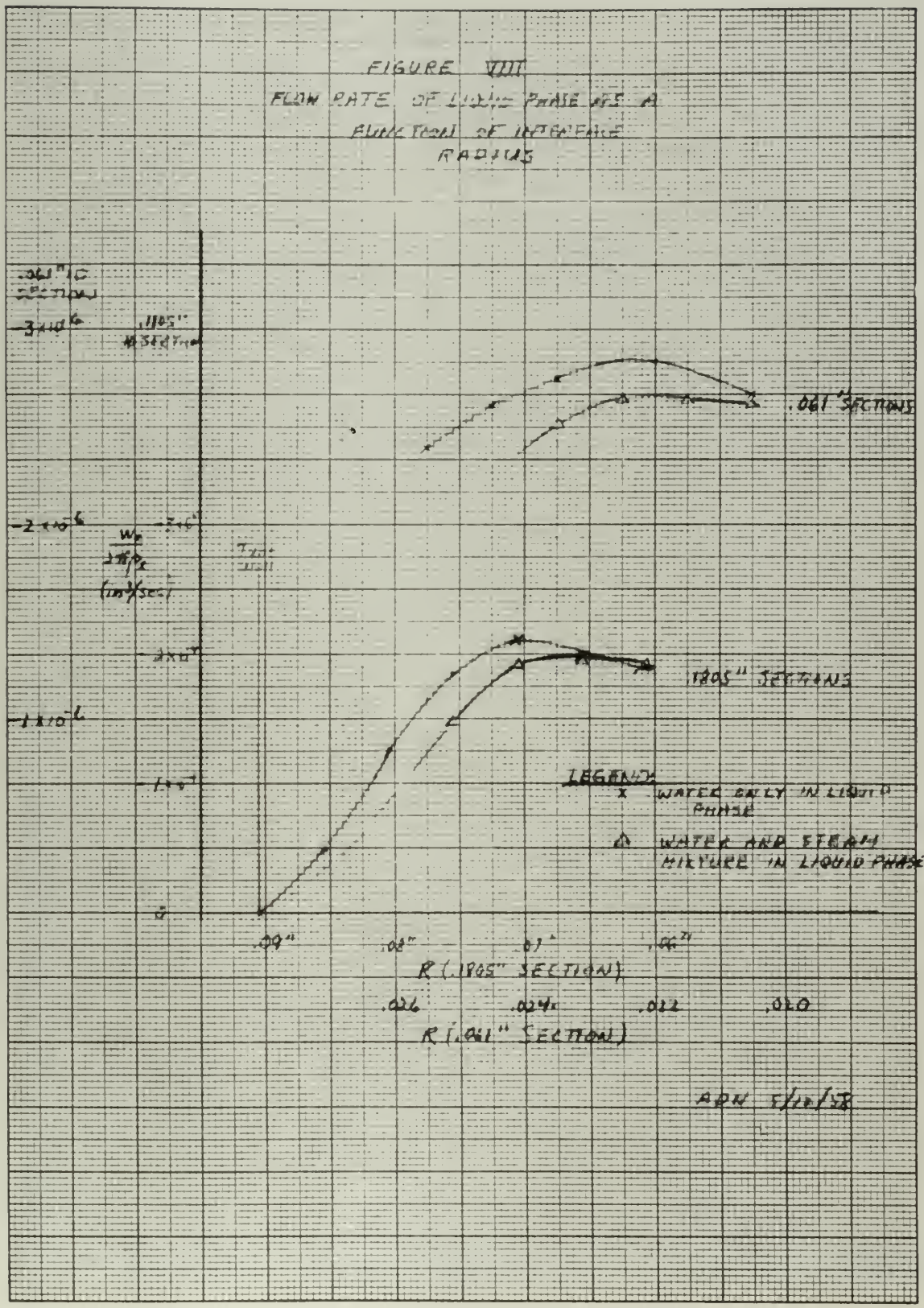

FIGURE VIII

FLOW RATE OF LIQUID PHASE AS A FUNCTION OF INTERFACE RADIUS

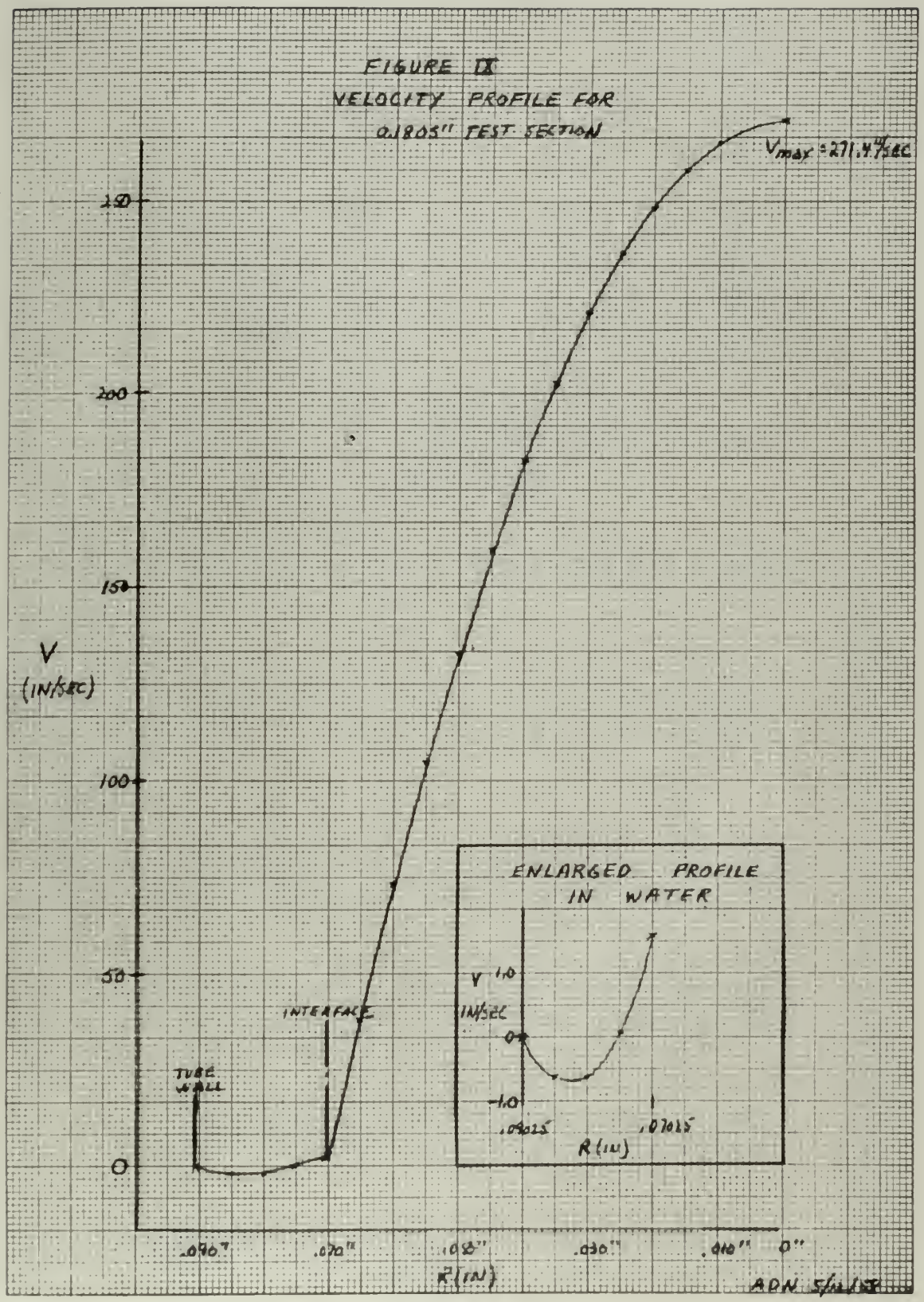
FIGURE IX
VELOCITY PROFILE FOR
0.1805" TEST SECTION
V_{max} = 271.4 IN/SEC
250
200
150
100
50
0
V
(IN/SEC)
ENLARGED PROFILE
IN WATER
V
IN/SEC
1.0
0
-1.0
.07025
.07075
R (IN)
INTERFACE
TUBE
WALL
.090"
.070"
.050"
.030"
.010"
0"
R (IN)
ADN 5/11/67

APPENDIX B

Data Tables

TABLE I

Runs with A Inch Test Section

Date	I (Amp)	E (Volts)	Watts	Thermocouple Reading (mv)	T_{ave} (°F)	Length of run (min.)	Remarks
3/12/58	277	.625	173	6.87	233	-	Decrease in power believed due to storage capacity of equipment
	265	.612	162	6.99	236	-	
	265	.610	162	6.86	233	-	
	255	.596	152	6.87	233	3	
	245	.568	140	6.[illegible]	233	13	Believed best on 3/12
	242	.567	137	6.94	235	15	
3/14/58	260	.600	156	6.90	234	78	
	260	.617	161	7.10	239	37	
	265	.627	166	6.95	235	19	
	265	.645	171	6.92	234	5	
	260	.612	159	6.62	227	13	
	259	.608	158	6.48	223	16	
	255	.630	161	6.56	226	2	
	255	.625	159	6.71	230	10	
	260	.607	158	6.54	225	19	
3/19/58	Equipment run for 30 minutes to warm up.						
	265	.629	167	7.10	239	17	Run used in T vs Time Plot
	263	.627	165	6.72	230	60	
			159		232		Average

Note: T_{ave} includes 3° allowance for mica insulating effect.

TABLE II

Runs with 6 inch Test Sections

Date	I (amp)	E (Volts)	Watts	Thermocouple Reading (mv)	T_{ave} (°F)	Length of run (min.)	Remarks
3/21/58	244	.995	243	6.29	218	16	Thermocouple readings low due to installation.
	248	1.025	252	6.42	222	21	
3/26/58	250	1.025	256	6.57	225	6	
	248	1.015	252	6.55	225	4	
			251		223		Average
3/27/58	Different 6 inch test section (#2) installed						
3/28/58	220	.970	216	6.54	224	9	
	214	.945	202	6.58	226	26	
	210	.930	195	6.55	225	12	
	210	.930	195	6.54	224	7	
3/31/58	220	.930	-	-	-	-	Cold equipment
	210	.935	196	6.57	225	17	
	214	.930	204	6.58	226	8	
	210	.935	195	6.61	227	4	
	210	.940	197	6.64	228	3	
	210	.938	197	6.66	229	3	
			200		227		Average

TABLE II (Cont.)

Date	I (amm)	E (Volts)	Watts	Thermocouple Reading (mv)	T_{ave} (°F)	Length of run (min.)	Remarks
4/10/58	Test section installed 3/27/58 (with modified throat).						
	230	?	-	-	-	-	Burnout on increase of I.
	228	1.015	232	6.56	225	6	
	230	1.03	237	6.61	227	2	
	228	1.03	235	-	-	-	
	226	1.005	227	-	-	-	
	224	.995	223	6.60	227	2	
	222	.980	218	6.53	224	8	
	227	1.005	228	6.58	226	9	Believed best run this day
	226	1.005	227	6.54	224	10	
			228		225		Average

Note: T_{ave} includes 3° allowance for mica insulating effect.

TABLE III

Runs with 10¾ inch Test Section

Date	I (amp)	E (Volts)	Watts	Thermocouple* Reading (mv)	T_{ave} (°F)	Length of run (min.)	Remarks
4/25/58	84.0	5.30	445	-	-	6	
	82.0	5.20	426	-	-	3	
	84.0	5.20	436	6.35	221	-	
			436		271		Average
	42.0	2.40	101		220		Dry - to estimate losses

TABLE IV

Runs with 8 inch Test Section

(Stainless steel with 0.061"I.D. and 0.125"O.D.)

Date	I (amp)	E (Volts)	Watts	Thermocouple* Reading (mv)	T_{ave} (°F)	Length of run (min.)	Remarks
4/30/58	10.5	.46	8.30	6.42	222	12	
5/ 1/58	20.0	.54	10.8	6.45	223	5	
	20.0	.52	10.4	6.47	223	2	
			9.9		223		Average

Note: T_{ave} includes 3° allowance for mica insulating effect.

---

*.35 mv has been added because of increased thickness of mica and installation of thermocouples as compared to data of Tables I and II.

TABLE V

Runs with A Inch Test Section

(Stainless steel with 0.061" I.D. and 0.125" O.D.)

Date	I (amp)	E (volts)	Watts	Thermocouple* Reading (mv)	T_{ave} (°F)	Length of run (min.)	Remarks
5/6/58	24.0	.33	7.92	6.50	224	7	
	24.0	.34	8.16	6.47	223	4	
			8.04		224		Average

Note: T_{ave} includes 3° allowance for mica insulating effect.

*0.35 mv has been added because of increased thickness of mica and installation of thermocouples as compared to data of Tables I and II.

Appendix A

References

1. Calegar, W. C., Stovall, T. D., and Huntington, R. L., "More Data on Two-Phase Vertical Flow", Petroleum Refiner, 33, November 1954, p. 209-211.

2. Jakob, M., Heat Transfer, Vol. I, J. Wiley & Sons, (1949).

3. Keenan, J. H., and Keyes, F. G., Thermodynamic Properties of Steam, J. Wiley & Sons, (1936).

4. McAdams, W. H., Heat Transmission, 3rd Ed., McGraw-Hill, (1954).

References

1. [illegible]
2. [illegible]
3. [illegible]
4. [illegible]

thesN444
Natural convection burnout in tubes clos
3 2768 001 89920 6
DUDLEY KNOX LIBRARY